Journal of the Serbian Chemical Society
JSCS-info@shd.org.rs • www.shd.org.rs/JSCS
J. Serb. Chem. Soc. 78 (1) 101–114 (2013) UDC 546.185–034.1+669.14+621.793:544.351.3
JSCS–4400 *Original scientific paper*

Determination of surface coverage of iron-phosphate coatings on steel using the voltammetric anodic dissolution technique

JOVAN P. POPIĆ[1#], BORE V. JEGDIĆ[2#], JELENA B. BAJAT[3#], MIODRAG MITRIĆ[4] and VESNA B. MIŠKOVIĆ-STANKOVIĆ[3#*]

[1]ICTM-Department of Electrochemistry, University of Belgrade, Njegoševa 12, Belgrade, Serbia, [2]Institute GOŠA, Milana Rakića 35, 11000 Belgrade, Serbia, [3]Faculty of Technology and Metallurgy, University of Belgrade, Karnegijeva 4, P. O. Box 3503, 11120 Belgrade, Serbia and [4]Vinča Institute of Nuclear Sciences, P. 0. Box 522, 11001 Belgrade, Serbia

(Received 6 July, revised 13 September 2012)

Abstract: In this study, the effect of deposition time and concentration of $NaNO_2$ in the phosphate bath on the surface morphology of iron-phosphate coatings on low carbon steel was investigated using scanning electron microscopy (SEM) and atomic force microscopy (AFM). The composition of iron-phosphate coatings was determined using energy dispersive X-ray spectroscopy (EDS) and X-ray diffraction (XRD), while surface coverage was evaluated by the voltammetric anodic dissolution (VAD) technique in the borate solution. The addition of $NaNO_2$ to the phosphate bath significantly increased the surface coverage since better packed crystals of smaller size, which favour the phosphate nucleation, were obtained. It was also shown that prolonged deposition time increased the surface coverage, coating roughness and crystal size in the lateral direction, altering also the crystal shape from large platelets non-uniformly distributed on the steel surface during the initial time to better-packed laminated and needle-like structures during prolonged exposure.

Keywords: low carbon steel; iron-phosphate coatings; surface coverage; VAD; AFM.

INTRODUCTION

Corrosion resistance of a metal/organic coating system largely depends on the pre-treatment of the metal surface prior to organic coating deposition. The pre-treatment of the metal surface usually includes degreasing of the metal and formation of a conversion coating on the surface with the aim of increasing the corrosion resistance and adhesion strength between metal and organic coating. In practice, zinc-phosphate coatings, manganese-phosphate coatings, zinc-manga-

* Corresponding author. E-mail: vesna@tmf.bg.ac.rs
# Serbian Chemical Society member.
doi: 10.2298/JSC120706096P

nese-phosphate coatings and zinc-calcium-phosphate coatings have usually been used as conversion coatings on steel, aluminium, magnesium and zinc.[1–9] Iron-phosphate coatings showed less corrosion stability in respect to zinc-phosphate coatings,[5,10–12] but together with top organic coatings, good corrosion protection of steel could be achieved.[11,13–19] It was shown that steel pre-treatment with an iron-phosphate coating increased the adhesion strength of the organic coating, as well as the corrosion stability of the protective system, as compared to organic coating on a bare steel substrate.[3,13,14] The advantages of iron-phosphate pre-treatment are the simple and cheap equipment and waste water treatment.

The quality of the iron-phosphate layers greatly depends on the fraction of the total surface area covered by the phosphate coating. Various factors affect the surface coverage, in particular the composition of the deposition bath, bath temperature, deposition time, the morphology of the deposit and additives (accelerators) used in the electrolyte.

Various types of chemical accelerators for phosphating can be used, such as sodium nitrite, nitrates and chlorates.[1,3–5,10–12] Previous research[20,21] indicated that iron-phosphate coatings on steel surface do not have great surface coverage. It was shown that the addition of formic acid, sodium chlorate, or sodium nitrobenzenesulphonate in the phosphating solution increased the surface coverage of phosphate coatings.[17,18,20,22]

The surface coverage of phosphate coatings is usually measured using electrochemical methods: polarization resistance measurements,[23–25] electrochemical impedance spectroscopy,[24–26] corrosion potential and corrosion current measurements.[24,27] The voltammetric anodic dissolution (VAD) technique,[28–30] as an electrochemical method for the determination of surface coverage, has been used lately. This technique is based on the dissolution and passivation of a coated or uncoated metal surface.

In this work, the surface morphology of iron-phosphate coatings deposited on low carbon steel was investigated as a function of the deposition time and concentration of $NaNO_2$ in the phosphating bath. The surface coverage of these coatings was quantitatively determined using the VAD method, with the aim of obtaining iron-phosphate coatings with the highest surface coverage and, consequently, with better corrosion stability.

EXPERIMENTAL

Sample preparation

Low carbon steel panels (50 mm×25 mm×0.8 mm) were used as the substrate for iron-phosphate coating deposition. The chemical composition of the low carbon steel was (wt. %): C, 0.119; Si, 0.019; Mn, 0.250; P, 0.019; S, 0.014; Cr, 0.012 and Ni, 0.019.

Prior to the deposition of the iron-phosphate coatings, the steel panels were polished with SiC papers #220, #400 and #600, degreased in 0.2 g dm^{-3} nonylphenol ethoxylate at room temperature for 5 min and rinsed with distilled water. The iron-phosphate coatings were

formed chemically by immersion in the phosphating bath containing 0.92 g dm^{-3} H_3PO_4, 0.34 g dm^{-3} NaOH and 0.125 g dm^{-3} nonylphenol ethoxylate at 50 °C for different times (from 30 s to 15 min). The iron-phosphate coatings were deposited on steel in the phosphating bath without or with the addition of $NaNO_2$ as an accelerator, at different concentrations: 0.1, 0.5 and 1.0 g dm^{-3}. All solutions were prepared with analytical grade chemical compounds and deionised water.

Surface coverage measurements

The surface coverage of the iron-phosphate coatings on low carbon steel was determined using the electrochemical voltametric anodic dissolution (VAD) technique, in which the passivation charge of the substrate is measured. The VAD was recorded in 0.3 mol dm^{-3} H_3BO_3 + borax ($Na_2B_4O_7 \cdot 10H_2O$), pH 7.6, with a potential sweep rate of 2 mV s^{-1} starting from the open circuit potential (OCP), using a GAMRY Reference 600 potentiostat–galvanostat/ZRA.

Borate solution was chosen because when immersed in this solution during anodic polarization, low carbon steel actively dissolves at potentials near to the corrosive ones,[31-33] while further polarization leads to steel passivation. In addition, it was stated in the literature[28] that iron-phosphate coatings do not dissolve in neutral solutions.

Surface morphology

The surface morphology of the bare steel and iron-phosphate coatings on steel was investigated by atomic force microscopy (AFM), operated in the contact mode under ambient conditions, at a scan rate 0.7 Hz, scan angle 0, scan points 256 and scan lines 256 using an Asylum model MFP-3D microscope.

The microstructure of the iron-phosphate coatings was examined by scanning electron microscopy (SEM) using a JSM-6390 LV (JEOL) instrument. The compositional analysis was realized using an energy dispersive spectroscopy (EDS) attachment on the scanning electron microscope.

XRD measurements

X-Ray diffraction (XRD) measurements were performed on a Philips PW 1050 powder diffractometer with Ni filtered CuK_α radiation (λ = 1.5418 Å) and a scintillation detector within the 15−80° 2θ range in 0.05° steps with a scanning time of 45 s per step. The quailtative analysis of the samples was performed by XRD analysis based on the identification of the peaks using commercially available EVA software (DIFFRACplus EVA). The phases were identified using the Powder Diffraction File (PDF) database (JCPDS, International Centre for Diffraction Data).

RESULTS AND DISCUSSION

Surface morphology

The surface morphology of iron-phosphate coatings was investigated using the SEM and AFM techniques, commonly used in analyzing the surface morphology of coatings.[34,35] Low carbon steel was phosphated for different times: 5, 10 and 15 min, with the aim of investigating the influence of deposition time on the morphology and composition of the iron-phosphate coatings. Fig. 1 shows The SEM microphotographs of the bare steel (a) and of the iron-phosphate coatings deposited at different times (b, c and d). The sporadic small spots on the

bare steel (Fig. 1a) are probably the result of mechanical damage during polishing. The different surface coverage of steel with iron-phosphate coatings deposited for different phosphating times can be seen in Figs. 1b–1d. Small crystal nuclei of the iron-phosphate coating sporadically emerged during a deposition time of 5 min, while bigger crystals grew during longer deposition times.

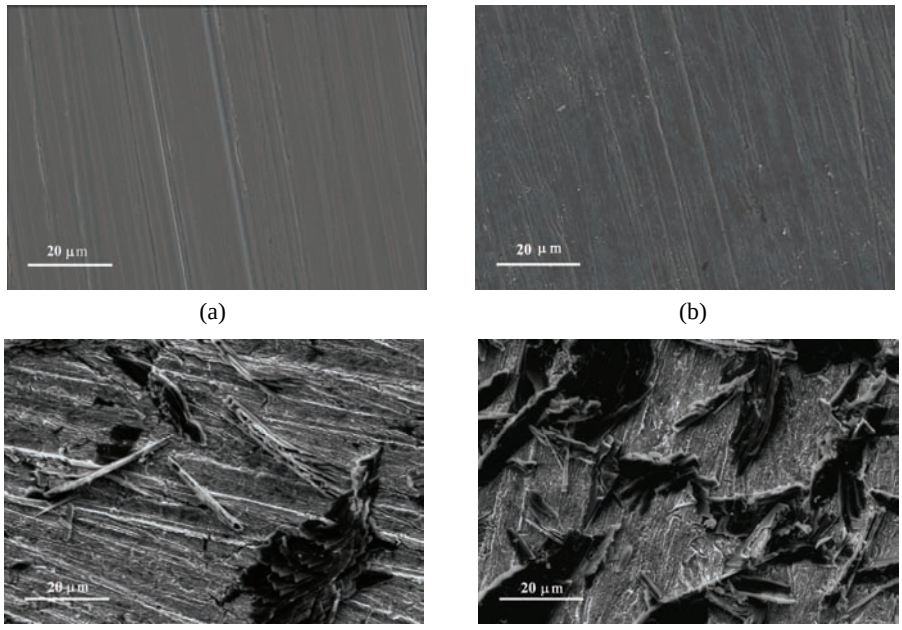

(a) (b)

(c) (d)

Fig. 1. Microphotographs of the steel surface prior to (a) and after phosphating for b) 5, c) 10 and d) 15 min.

The iron-phosphate crystals in the shape of platelets, non-uniformly distributed on the steel surface were obtained during a deposition time of 5 min (not shown). Their grain size, estimated by AFM, was 3–9 µm, while longer deposition times favoured lateral crystal growth of up to 15 µm during 15 min (Fig. 2 and Table I). Based on several AFM measurements on different surface spots, it could be observed that during prolonged deposition, the crystals grew in the normal direction only up to 1.2 µm in height, regardless of the deposition time. The values of surface roughness (*RMS*), derived from AFM images, are presented in Table I. The *RMS* value for the polished bare steel was 55 nm, while the *RMS* values of the iron-phosphate coatings deposited up to 10 min significantly increased to 280 nm. The observed increase in roughness is the result of the nucleation and growth of iron-phosphate crystals on the steel surface with prolonged

deposition time. It could also be noticed that the values of the *RMS* did not significantly change deposition times longer than 10 min were employed.

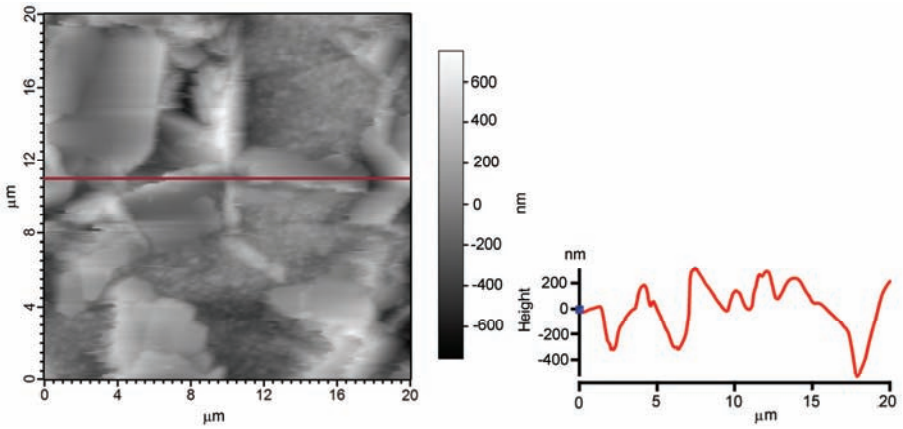

Fig. 2. AFM Image and height profile of the iron-phosphate coating on steel deposited during 15 min.

TABLE I. The values of *RMS*, grain size, passivation current, i_p, passivation charge density, Q_{pass}, surface coverage, Θ, and composition of the iron-phosphate coatings deposited with and without $NaNO_2$ in the plating bath

Substrate	Deposition time, min	$c(NaNO_2)$ g dm^{-3}	*RMS* nm	Grain size range µm	I_p µA cm^{-2}	Q_{pass} mC cm^{-2}	Θ %	Concentration at. %		
								O	P	Fe
Bare steel	–	–	55	–	294	12.3	0	–	–	–
Iron-phosphate coating	5	0	215	3–9	208	9.14	26.1	2.05	1.03	96.92
		0.1	–	–	122	5.48	55.3	–	–	–
		0.5	147	4–6	110	4.96	59.5	7.88	4.67	80.14
		1.0	–	–	95	4.30	64.9	–	–	–
	10	0	280	4–10	161	7.58	38.2	3.41	2.66	93.93
	15	0	270	5 –15	149	7.26	40.8	5.87	3.66	90.46

The EDS measurements provided information about the concentrations of particular elements on the surface of the phosphate coatings. The EDS spectra showed that the iron-phosphate coatings contained iron, oxygen and phosphorus. The semi-quantitative elemental compositions, obtained from the EDS analysis, are given in Table I. It could be noticed that the concentrations of oxygen and phosphorus increased with increasing deposition time, while that of iron decreased, indicating the growth of phosphate coatings with longer deposition time.

The phase composition of iron-phosphate coatings was determined by XRD analysis (Fig. 3). The phases present in the phosphate layers were mainly $FePO_4$ (according to PDF No. 01-072-2124 (ICSD 040863)), Fe_2O_3 (according to PDF

No. 00-052-1449) and Fe_3O_4 (according to PDF No. 01-079-0416 (ICSD 065338)).

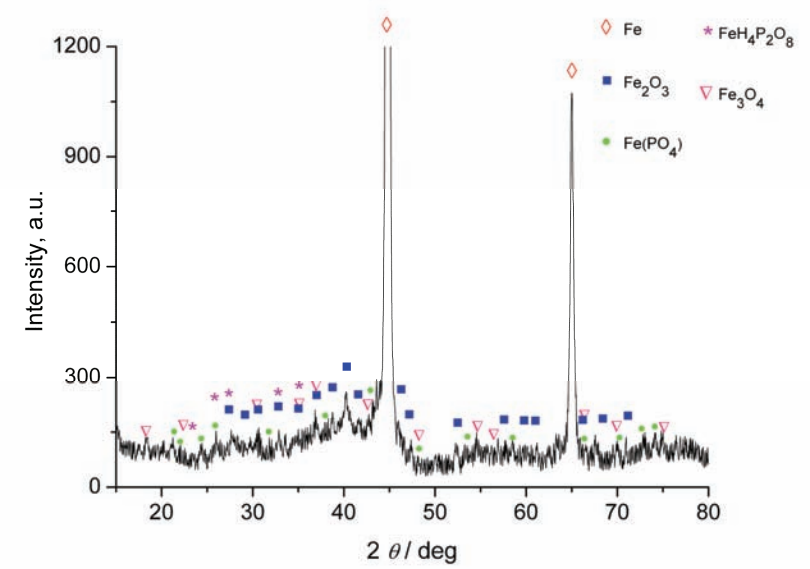

Fig. 3. XRD Pattern of an iron-phosphate coating on steel (deposition time: 5 min).

The formation of iron phosphate coating on steel occurs through reactions (1) and (2).[8] NaH_2PO_4 is formed from the H_3PO_4 and NaOH present in the plating bath:

$$Fe + 8NaH_2PO_4 + 4H_2O + 2O_2 \rightarrow 4Fe(H_2PO_4)_2 + 8NaOH \quad (1)$$

$$2Fe(H_2PO_4)_2 + 2NaOH + 1/2O_2 \rightarrow 2FePO_4 + 2NaH_2PO_4 + 3H_2O \quad (2)$$

In parallel, in the presence of oxygen (from the water-based phosphating bath), metallic iron is oxidized and $Fe(OH)_2$ and $Fe(OH)_3$ are formed on the iron surface. Iron hydroxides change gradually to iron oxide, Fe_2O_3 and Fe_3O_4, resulting in the formation of a passive film on the steel.[36]

Based on the AFM results, it could be concluded that two types of phosphate crystals were formed on the steel surface immersed in the phosphating solution: platelets, during initial deposition time, and laminated and needle-like crystals, during prolonged deposition times. The growth of iron-phosphate crystals starts with heterogeneous nucleation on the steel surface. Initially, the phosphate crystals grow in both the normal and lateral directions. During prolonged deposition, the crystals grow in the normal direction only up to 1.2 μm, regardless of the deposition time. Longer deposition times favour lateral crystal growth, up to 15 μm for a deposition time of 15 min (Table I). Extension of the phosphating time also

leads to the nucleation and growth of new crystals on the steel surface. In this way, longer deposition times result in greater surface coverage (Figs. 1 and 2) and greater amounts of phosphate deposit were obtained with greater amounts of oxygen and phosphorus, determined by EDS analysis (Table I). However, the iron-phosphate coating formed on the low carbon steel was not compact and the coating was significantly porous even after 15 min of phosphating.

Surface coverage

The surface coverage of iron-phosphate coatings on steel was determined by the VAD method in borate solution. Several solutions were tested but the borate solution was the most suitable. Namely, during anodic polarization in borate solution, steel is dissolved at potentials around the corrosion potentials, and during further polarization steel passivated.

Since the iron-phosphate coatings on steel contain iron phosphate and iron oxide,[5,8] their dissolubility in neutral borate solutions becomes questionable. However, bearing in mind that the rate of dissolution of Fe_2O_3 in slightly acidic and neutral solutions is very low,[20,31,33,37] this solution was adequate. Ptacek *et al.*[20] also showed that the rate of iron phosphate dissolution in slightly acidic solutions is very low. Thus, it was concluded that VAD method in borate solution could be used to determine the surface coverage of iron-phosphate coatings on steel.

Anodic polarization curves for bare steel and steel with iron-phosphate coatings in borate solution are shown in Fig. 4. During the anodic polarization of bare steel, the current passivation peak occurred at a potential of around –0.55 V.

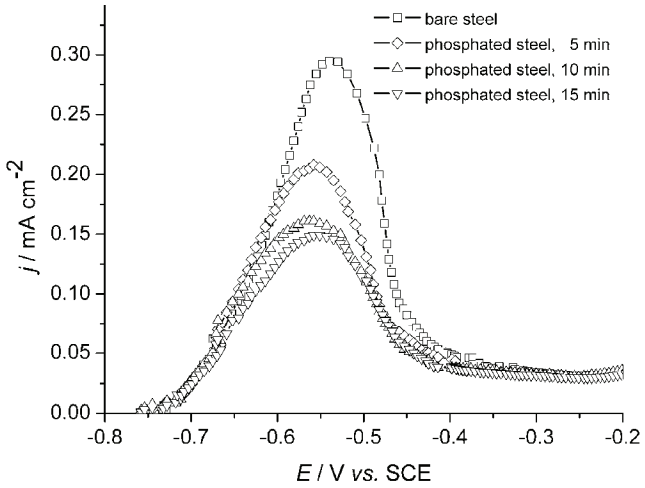

Fig. 4. Voltammetric anodic dissolution (VAD) curves in borate solution (pH 7.6) for bare steel and iron-phosphate coatings on steel, deposited during different deposition times.

The iron-phosphate coatings decreased the anodic dissolution of steel, as well as the anodic current passivation peaks (i_p). Increasing the coating deposition time resulted in decreased anodic dissolution of the steel. The values of anodic current passivation peaks, determined from VAD measurements for each phosphating condition, are given in Table I. The amount of passivation charge density (Q_{pass}) was calculated based on the measured experimental data, *i.e.*, from the value of the current of the anodic dissolution from the corrosion potential to the passivation peak and the duration of anodic dissolution until the passivation peak. Passivation charge density for bare steel surface was 12.26 mC cm^{-2}. This charge is defined as Q°_{pass} (the standard passivation charge density). The formation of the iron-phosphate coating on the steel surface led to a decrease in Q_{pass}.

Comparison of the passivation charge density of the bare substrate, Q°_{pass}, and that of the coated substrate, Q_{pass}, supplies the surface coverage, which is expressed by:

$$\Theta = 1 - \frac{Q_{pass}}{Q^{\circ}_{pass}} \quad (1)$$

where Θ is surface coverage, or the fraction of substrate area covered by the coating.

The values of the passivation charge density and surface coverage by the iron-phosphate coatings obtained during different phosphating times are given in Table I.

Based on the results presented in Fig. 4 and Table I, it could be concluded that the surface coverage by an iron-phosphate coating on the steel surface was greater when the deposition time was longer. The surface coverage by the iron-phosphate coating formed on the steel surface during 5 min was very low (26.1 %). A longer deposition time (10 min) resulted in increased surface coverage of iron-phosphate coating and the highest surface coverage (40.8 %) was obtained with the longest deposition time (15 min). It should be noted that even the highest surface coverage of 40.8 % is not actually significant, especially bearing in mind the long deposition time. The results of the electrochemically obtained surface coverage measurements (Fig. 4) are in a good agreement with the morphology of iron-phosphate coatings, shown in Figs. 1 and 2. This means that the application of the fast electrochemical method can very precisely determine the surface coverage of the iron-phosphate coating on the steel surface.

The effect of $NaNO_2$

Different amounts of $NaNO_2$ were added to the phosphating bath with the aim of accelerating the formation process of iron-phosphate coatings and obtaining better surface coverage by the deposited coatings. The anodic polarization

curves in borate solution are shown in Fig. 5. The obtained values of anodic current passivation peaks, passivation charge density and the surface coverage of the iron-phosphate coatings are given in Table I.

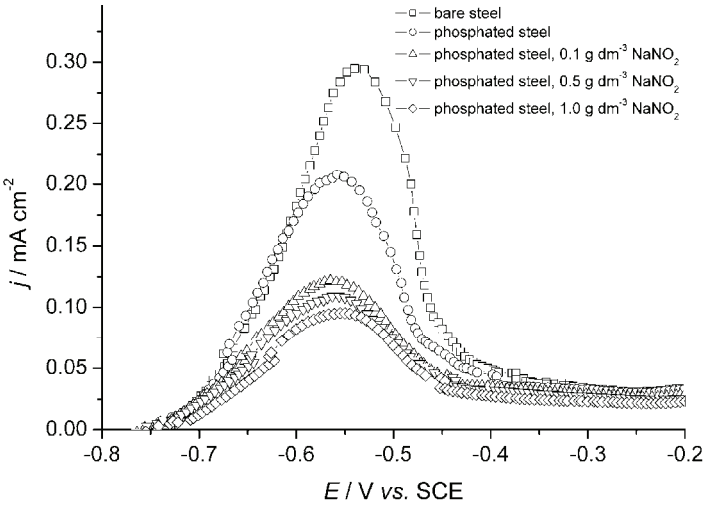

Fig. 5. Voltammetric anodic dissolution (VAD) curves in borate solution (pH 7.6) for bare steel and iron-phosphate coatings on steel deposited during 5 min without and with different concentrations of $NaNO_2$ in the plating bath.

Based on these results, it could be concluded that the addition of $NaNO_2$ to the phosphate solution significantly increased the surface coverage. Even a small amount of $NaNO_2$ (0.1 g dm^{-3} $NaNO_2$) in the plating bath increased the surface coverage from 26.1 to 55.3 % (Table I). On increasing the $NaNO_2$ concentration in the bath resulted in even higher surface coverage. The highest surface coverage (64.9 %) was obtained with 1.0 g dm^{-3} $NaNO_2$ in the bath. A concentration of 0.5 g dm^{-3} was chosen for further examination for both economical and environmental reasons, since the surface coverage did not significantly increase when the concentration of $NaNO_2$ was increased from 0.5 to 1.0 g dm^{-3}.

In order to monitor the nucleation and initial growth of iron-phosphate coatings deposited having $NaNO_2$ in the bath, the morphology of the coatings deposited from a bath with 0.5 g dm^{-3} of $NaNO_2$ during different times was analyzed (Fig. 6). It is evident that even after 0.5 min, centres of phosphate crystal nucleation had been formed (Fig. 6b). Extending the phosphating time to 1.0 min caused further growth of the single phosphate crystals (Fig. 6c). After 5.0 min of phosphating, the whole surface was covered with phosphate crystals. The iron-phosphate coatings deposited on the steel surface were mixtures of laminated and

needle-like structure, the needle-like structure of phosphate crystals being dominant (Fig. 6d).

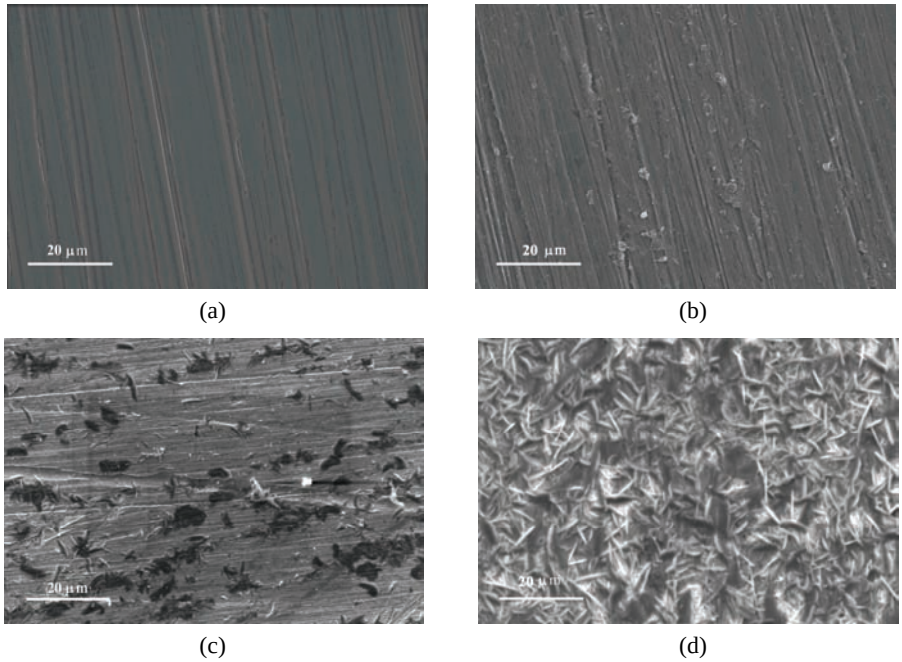

(a) (b)

(c) (d)

Fig. 6. Microphotographs of the steel surface prior to (a) and after phosphating with 0.5 g dm^{-3} $NaNO_2$ in the plating bath for b) 0.5, c) 1 and d) 5 min.

The EDS spectrum showed that iron-phosphate coating formed in the phosphate bath with $NaNO_2$ during 5 min contained iron, oxygen and phosphorus. The concentrations of the individual elements are presented in Table I (blank cells in Table I are for the samples where EDS analysis was not performed). Comparing these results with the results obtained for the iron-phosphate coatings deposited during the same time without the accelerator in the bath (Table I), it could be concluded that a significant increase in the concentration of phosphorus on the steel surface (nearly five times greater) was accomplished with the accelerator in the phosphating bath.

The values of the *RMS* and grain size of the iron-phosphate deposits obtained in the phosphating bath with 0.5 g dm^{-3} $NaNO_2$ for different phosphating time are presented in Table II. The AFM of the iron-phosphate coating confirmed that the centres of phosphate nucleation had been formed on the steel surface already after 30 s of phosphating. The size of formed phosphate nuclei were 0.3––0.7 μm (Table II). The surface roughness remained unchanged as compared to

that of the bare steel surface (52 nm, Table II). Extension of the phosphating time to 60 s led to an increase in the size of the phosphate crystals, which were as large as 3 μm. These crystals did not have a defined form and they were dispersed over the steel surface covering 20–30 % of the surface area. The surface roughness was increased and had a value of 127 nm. Further extension of the phosphating time to 5 min significantly increased the amount of phosphate crystals. The structure of these crystals could be defined as mostly laminated and needle-like structures with a size of the crystal ranging from 4 to 6 μm. Surface roughness has been slightly increased and amounts 147 nm.

TABLE II. The values of *RMS* and grain size of bare steel and iron-phosphate coatings on steel deposited with 0.5 g dm^{-3} $NaNO_2$ in the plating bath for different deposition times

Substrate	Deposition time, min	*RMS* / nm	Grain size range, μm
Bare steel	–	55	–
Iron-phosphate coating	0.5	52	0.3–0.7
	1.0	127	2–3
	5.0	147	4–6

Based on these results, it could be concluded that the presence of the accelerator $NaNO_2$ in the iron-phosphating bath resulted in a faster nucleation of phosphate crystals. The size of these crystals was smaller in comparison to those obtained in the phosphating solution without an accelerator. These results suggest that the $NaNO_2$ causes a decrease in the crystal size. Namely, the smaller crystal size obtained in the bath with $NaNO_2$ indicates that this additive has an effect on surface activation, favouring phosphate nucleation and leading to the formation of smaller crystals. In the presence of the accelerator, the concentration of phosphate crystals on the steel surface increased and crystals were more tightly packed. In addition, the roughness of the iron-phosphate coating decreased (Tables I and II). The higher concentration of phosphate crystals on the steel surface leads to an increase in the surface coverage of the iron-phosphate coating.

The higher surface coverage of iron-phosphate coatings on steel deposited with 0.5 g dm^{-3} $NaNO_2$ in the plating bath during 5 min is also shown in Fig. 5 and Table I. It was not only higher than the surface coverage of iron-phosphate coating deposited from the $NaNO_2$-free plating bath during the same deposition time, but also much higher even than the surface coverage of the iron-phosphate coating deposited from the $NaNO_2$-free plating bath during 15 min (Table I). Thus, based on all the presented results, it could be concluded that the addition of 0.5 g dm^{-3} $NaNO_2$ in the plating bath resulted in the completely different surface morphology of iron-phosphate coating on steel (Figs. 1b and 6d) of better surface coverage. Similar conclusions can be found in the literature for zinc-phosphate coatings on steel when $NaNO_2$ was used as an accelerator.[4,5,20,26,30,38–41]

CONCLUSIONS

It was shown that the growth of the phosphate crystals in both the normal and lateral direction, monitored by AFM, SEM and EDS, started with heterogeneous nucleation on the steel surface. The phosphate crystals, in the shape of platelets non-uniformly distributed on the steel surface, were formed during the initial deposition time in a $NaNO_2$-free bath. Extension of the phosphating time resulted in the formation of phosphate crystals with laminated and needle-like structures of increased roughness and increased phosphorous concentration, because of crystals growth. Consequently, the surface coverage determined from current passivation increased with prolonged deposition time. The addition of $NaNO_2$ to the phosphate solution significantly increased the surface coverage. The so-obtained crystals were of smaller size and more densely packed, which resulted in decreased coating roughness. They had laminated and needle-like structure with the needle-like structure prevailing, as compared to the platelets shape of the crystals obtained from a $NaNO_2$-free bath. Smaller crystal size indicates that this additive ($NaNO_2$) had an effect on surface activation, favouring phosphate nucleation and leading to the formation of smaller and better packed crystals.

Acknowledgement. This research was financed by the Ministry of Education, Science and Technological Development of the Republic of Serbia, Grant III 45019. The authors would like to thank Yao Xiong, Ph.D. student, Institute for Corrosion and Multiphase Technology, Ohio University, OH, USA, for helping in the AFM analyses, and Sanja Eraković, PhD student, Faculty of Technology and Metallurgy, University of Belgrade, for helping in the XRD analyses.

И З В О Д

ОДРЕЂИВАЊЕ ПОКРИВЕНОСТИ ПОВРШИНЕ ЧЕЛИКА ГВОЖЂЕ-ФОСФАТНИМ ПРЕВЛАКАМА АНОДНИМ РАСТВАРАЊЕМ ПРИМЕНОМ ЛИНЕАРНЕ ВОЛТАМЕТРИЈЕ

ЈОВАН П. ПОПИЋ[1], БОРЕ В. ЈЕГДИЋ[2], ЈЕЛЕНА Б. БАЈАТ[3], МИОДРАГ МИТРИЋ[4] и ВЕСНА Б. МИШКОВИЋ-СТАНКОВИЋ[3]

[1]ИХТМ – Центар за електрохемију, Универзитет у Београду, Његошева 12, Београд, [2]Институт ГОША, Милана Ракића 35, 11000 Београд, [3]Технолошко–металуршки факултет, Универзитет у Београду, Карнегијева 4, 11120 Београд и [4]Институт за нуклеарне науке Винча, Универзитет у Београду, п. пр. 522, Београд

У овом раду је, применом скенирајуће електронске микроскопије (SEM) и микроскопије међуатомских сила (AFM), испитиван утицај времена таложења и концентрације $NaNO_2$ у раствору за фосфатирање на морфологију гвожђе-фосфатних превлака на ниско-угљеничном челику. Састав гвожђе–фосфатних превлака је одређен применом енергетске дисперзионе атомске анализе (EDS) и дифракцијом X-зрака (XRD), док је покривеност површине одређивана анодним растварањем у боратном раствору применом линеарне волтаметрије (VAD). Показано је да додатак $NaNO_2$ у раствору за фосфатирање значајно повећава покривеност површине челика, јер се формирају боље паковани кристали, мање величине. Дуже време таложења такође повећава покривеност површине, као и храпавост превлаке и ширину кристала. Облик кристала се током дужег

времена таложења мења од кристала у облику већих плоча неуниформно распоређених на површини челика, ка боље пакованим ламинарним и игличастим кристалима.

(Примљено 6. јула, ревидирано 13. септембра 2012)

REFERENCES

1. A. Losch, E. Klusmann, J. W. Schultze, *Electrochim. Acta* **39** (1994) 1183
2. L. Fedrizzi, F. Deflorian, S. Rossi, L. Fambri, P. L. Bonora, *Prog. Org. Coat.* **42** (2001) 65
3. E. P. Banczek, P. R. P. Rodrigues, I. Costa, *Surf. Coat. Technol.* **202** (2008) 2008
4. E. P. Banczek, P. R. P. Rodrigues, I. Costa, *Surf. Coat. Technol.* **201** (2006) 3701
5. ASM Handbook, *Corrosion, Fundamentals, Testing, and Protection*, Vol. 13A, ASM International, OH, USA, 2005, p. 712–720
6. S. Q. Xu, Q. Li, Y. H. Lu, B. Chen, J. M. Fan, *Surf. Eng.* **26** (2010) 328
7. X. M. Song, G. Yu, H. B. Yi, L. Y. Ye, B. N. Hu, *Surf. Eng.* **26** (2010) 371
8. C. M. Wang, W. T. Tsai, Y. P. Lee, *Surf. Eng.* **24** (2008) 392
9. H. Nikdehghan, A. Amadeh, A. Honarbakhsh-Raouf, *Surf. Eng.* **24** (2008) 287
10. T. Biestek, J. Weber, *Electrolytic and chemical conversion coatings*, Portcullis Press, Redhill, Surrey, 1976, p. 180
11. B. Tepe, B. Gunay, *Prog. Org. Coat.* **62** (2008) 134
12. I. I. Hain, *Teoriya i praktika fosfatirovaniya metallov*, Himiya, Moskva, 1973, p. 68 (in Russian)
13. J. B. Bajat, V. B. Mišković-Stanković, J. P. Popić, D. M. Dražić, *Prog. Org. Coat.* **62** (2008) 201
14. B. V. Jegdić, J. B. Bajat, J. P. Popić, S. I. Stevanović, V. B. Mišković-Stanković, *Corr. Sci.* **53** (2011) 2872
15. L. Fedrizzi, E. J. Rodriguez, S. Rossi, F. Deflorian, *Prog. Org. Coat*. **46** (2003) 62
16. R. D. Armstrong, A. T. A. Jenkins, B. W. Johnson, *Corros. Sci*. **37** (1995) 1615
17. G. Gorecki, *Metal Finish*. **93** (1995) 36
18. G. Gorecki, *Corrosion* **48** (1992) 613
19. A. Albu-Yaron, Y. M. Aravot, *Thin Solid Films*, **232** (1993) 208
20. B. Ptacek, F. Dalard, J. J. Rameau, *Surf. Coat. Technol*. **82** (1996) 277
21. G. W. Critchlow, P. W. Webb, C. J. Tremlett, K. Brown, *Int. J. Adhes. Adhes*. **20** (2000) 113
22. C. Rajagopol, V. Subramanyan, V. Ramakishnan, K. Balakrishnan, *Paint India* **36** (1986) 16
23. D. Wang, P. Jokiel, A. Uebleis, H. Boehni, *Surf. Coat. Technol*. **88** (1996) 147
24. V. F. C. Lins, G. F. A. Reis, C. R. Aranja, T. Matencio, *Appl. Surf. Sci.* **253** (2006) 2875
25. L. Kwiatowski, *Surf. Eng.* **20** (2004) 292
26. A. Losch, J. W. Schultze, *J. Electroanal. Chem.* **359** (1993) 39
27. I. M. Notter, D. R. Gabe, *Corr. Sci.* **34** (1993) 851
28. H. A. Ponte, A. M. Maul, E. A. Alvarenga, *Mater. Res.* **5** (2002) 439
29. H. A. Ponte, A. M. Maul, *J. Appl. Electrochem.* **32** (2002) 641
30. E. P. Banczek, P. R. P. Rodrigues, I. Costa, *Surf. Coat. Technol.* **203** (2009) 1213
31. H. Kaesche, *Corrosion of metals*, Springer, Berlin, 2003, p. 209
32. N. Sato, M. Cohen, *J. Electrochem. Soc.* **111** (1964) 512
33. J. O' M. Bockris, D. M. Dražić, A. R. Despić, *Electrochim. Acta* **4** (1961) 325

34. G. Orhan, G. G. Gezdin, *J. Serb. Chem. Soc.* **77** (2012) 651
35. J. B. Bajat, S. Stevanović, B. M. Jokić, *J. Serb. Chem. Soc.* **76** (2011) 1537
36. H. Tamura, *Corros. Sci.* **50** (2008) 1872
37. P. E. Tegehall, N. G. Vannerberg, *Corros. Sci.* **32** (1991) 635
38. K. Ravichandran, H. Sivanandh, S. Ganesh, T. S. N. Sankara Narazanan, *Metal Finish.* **98** (2000) 48
39. G. Li, L. Niu, J. Lian, Z. Jiang, *Surf. Coat. Technol.* **176** (2004) 215
40. F. Fang, J. Jianf, S. Y. Tan, A. Ma, J. G. Jiang, *Surf. Coat. Technol.* **204** (2010) 2381
41. E. Klusmann, J. W. Schultze, *Electrochim. Acta* **48** (2003) 3325.